Mott-Kondo insulator behavior in the iron oxychalcogenides

B. Freelon,[1,2,*] Yu Hao Liu,[1] Jeng-Lung Chen,[1,3] L. Craco,[4,†] M. S. Laad,[5] S. Leoni,[6] Jiaqi Chen,[7] Li Tao,[7] Hangdong Wang,[7] R. Flauca,[8] Z. Yamani,[8] Minghu Fang,[7] Chinglin Chang,[3] J.-H. Guo,[1] and Z. Hussain[1]

[1]*Advanced Light Source Division, Lawrence Berkeley National Laboratory, One Cyclotron Road, Berkeley, California 94720, USA*

[2]*Advanced Photon Source, Argonne National Laboratory, Argonne, Illinois 60439, USA*

[3]*Department of Physics, Tamkang University, Tamsui, Taiwan 250*

[4]*Instituto de Física, Universidade Federal de Mato Grosso, 78060-900, Cuiabá, MT, Brazil*

[5]*The Institute of Mathematical Sciences, C.I.T. Campus, Chennai 600 113, India*

[6]*School of Chemistry, Cardiff University, Cardiff, CF10 3AT, United Kingdom*

[7]*Department of Physics, Zhejiang University, Hangzhou 310027, People's Republic of China*

[8]*Canadian Neutron Beam Centre, National Research Council, Chalk River Laboratories, Chalk River, Ontario K0J 1J0, Canada*

(Received 27 November 2014; revised manuscript received 9 September 2015; published 23 October 2015)

We perform a combined experimental-theoretical study of the Fe-oxychalcogenides (FeO*Ch*) series $La_2O_2Fe_2OM_2$ (M = S, Se), which are among the latest Fe-based materials with the potential to show unconventional high-T_c superconductivity (HTSC). A combination of incoherent Hubbard features in x-ray absorption and resonant inelastic x-ray scattering spectra, as well as resistivity data, reveal that the parent FeO*Ch* are correlation-driven insulators. To uncover microscopics underlying these findings, we perform local density approximation-plus-dynamical mean field theory (LDA+DMFT) calculations that reveal a novel Mott-Kondo insulating state. Based upon good agreement between theory and a range of data, we propose that FeO*Ch* may constitute an ideal testing ground to explore HTSC arising from a strange metal proximate to a novel selective-Mott quantum criticality.

DOI: 10.1103/PhysRevB.92.155139 PACS number(s): 74.70.Xa, 74.25.F−, 74.25.Jb

I. INTRODUCTION

Since the discovery [1] of high-temperature superconductivity (HTSC) in iron pnictides (FePn), a fundamental question has been whether the iron pnictides are weakly correlated metals or bad metals in close proximity to Mott localization [2,3]. These competing ideas must imply very different mechanisms of Fe-based HTSC. The Mottness view proposes that strong, orbitally selective electron correlation is relevant to HTSC, while the competing itinerant view holds that antiferromagnetic (AFM) order and superconductivity (SC) originate from a Kohn-Luttinger-like Fermi surface (FS) nesting mechanism with weak electronic correlations [4]. Early insights suggested the importance of varying the strength [2,5] of electron correlations using chemical substitutions to understand the relevance of Mott localization to iron HTSC. Since then, more evidence has accumulated in support of this proposal; FeSe is a bad metal without AF order [6], while parent Fe-oxychalcogenides are electrical insulators [7,8].

Most pnictide superconductors exhibit bad-metal normal states with hints of novel quantum criticality. The discovery of HTSC in alkaline iron selenides $A_{1-x}Fe_{2-y}Se_2$, where A = K, Tl, Cs, and Rb (referred to as "'245s") intensified this basic debate, because SC with $T_c = 30$ K emerges from doping an AFM insulating state occurring due to Fe-vacancy induced band narrowing [9]. Studying more of such materials to further develop a complete description of the general electronic phase diagram of iron superconductors is warranted. With this in mind, we investigated iron oxychalcogenides such as $X_2OFe_2O_2M_2$ [X = (La, Na, Ba), (M = (S, Se)] [10] because of (i) their similarities to LaFeOAs (1111) materials and (ii) the opportunity to study materials with slightly larger electron correlation than the pnicitides [7]. Moreover, $La_2O_2Fe_2OM_2$ (M = S, Se) offer the option to tune the strength of electronic correlations through disorder-free chalcogen exchange of S and Se. The FeO*Ch* consist of stacked double-layered units La_2O_2 and $Fe_2O(S,Se)_2$ as shown in Appendix A. The $Fe_2O(S,Se)_2$ unit contains an Fe-M layer that is similar to the FeAs layer in the pnictides. The rare-earth layer also contains an additional O(1) atom. Chalcogen substitution results in a slightly expanded Fe-square-lattice unit cell of $La_2O_2Fe_2OM_2$ compared to that of LaOFeAs [10]. The consequent decrease in the electronic bandwidth W increases the Hubbard U, offering a parameter to subtly vary U/W across a critical value for a Mott insulator phase.

In this paper, we first substantiate this reasoning by presenting measurements of the unoccupied and occupied Fe and oxygen density of states (DOS) obtained by soft x-ray absorption (XAS) and resonant inelastic x-ray scattering (RIXS). Strong Fe moment localization that can be tuned with chalcogen replacement, and, more crucially, the observation of incoherent Fe spectral weight due to Hubbard band formation marks the FeO*Ch* as correlation-driven insulators. The incoherent spectral weight undergoes a resonant enhancement in both the RIXS data and the lower Hubbard band (LHB) spectral weight analysis, indicating the Mott insulating character of both $La_2O_2Fe_2OS_2$ and $La_2O_2Fe_2OSe_2$. In addition, we show that these materials are orbital-selective Mott-Kondo insulators (MKI) [11]. We discuss how these findings imply HTSC arising from an incoherent metal proximate to novel selective-Mott quantum criticality.

*freelon@mit.edu

†lcraco@fisica.ufmt.br

II. EXPERIMENTAL

We investigated well-characterized $La_2O_2Fe_2OM_2$ M = (S, Se) polycrystalline materials, with nominal compositions, that were fabricated using solid-state reaction methods described earlier [7]. High purity La_2O_3, Fe, and (S, Se) powders were used as starting materials and laboratory x-ray and neutron powder diffraction data showed that these materials were single phase in agreement with the literature [12].

XAS and RIXS spectra for the FeO Ch were collected in a polarization averaged condition. In order to reduce the possibility of oxidation, iron oxychalcogenide samples were sheared under a pressure of 10^{-6} Torr in a pre-chamber immediately before being placed in the ultrahigh vacuum experimental chamber. All presented x-ray measurements were performed in the paramagnetic (PM) state above 150 K. The advanced light source beamlines 7.0.1 and 8.0.1 delivered x-ray beams of 100 micron spot sizes and energy resolutions of 0.2 eV (0.2 eV) and 0.5 eV (0.6 eV) for oxygen(iron) x-ray absorption and emission, respectively. The oxygen K-edge XAS intensity is proportional to the unoccupied p-weighted DOS resulting from the $\Delta l = \pm 1$ dipole selection rule for x-ray photon absorption. If the Fe-O related bond is partially covalent, O $2p$ states hybridize with Fe $3d$ orbitals and hence the pre-threshold for absorption, i.e., the low-energy fine structure, reveals itself in ligand-to-metal charge transfer excitations [13]. XAS is sensitive to metal atom coordination geometry and $3d$ occupation (oxidation state).

III. RESULTS: RIXS

Figure 1(a) shows the O K XAS profiles of $La_2O_2Fe_2OM_2$ (M = S, Se). The oxygen pre-edge feature at 530 eV has different intensities for M = S and Se. This aspect of the XAS data is reminiscent of doped pnictide spectra in which the 530-eV absorption feature evolves as a function of charge doping [14]. Here we focus on the energy regime near the absorption edge in order to investigate RIXS processes. O $K\alpha$-edge RIXS spectral data obtained using incident x-ray energies of 532 and 534 eV are presented in Fig. 1(b). The prominent peak is due to nonhybridizing O $2p$ states referred to as the oxygen main band peak. In addition, the oxygen RIXS spectra of $La_2O_2Fe_2OS_2$ contain a high-energy peak located to the left of the main band peak. Oxygen projected density function theory (DFT) calculations indicate that this spectral weight is due to O(2) atoms located in the Fe plane (see Ref. [7]). Based on this, we assign the high-energy O $K\alpha$-edge RIXS intensity observed in $La_2O_2Fe_2OS_2$ (522 eV) to oxygen states bonded to Fe states that form a LHB (see below). The striking absence of such a high-energy feature in the oxygen RIXS data of $La_2O_2Fe_2OSe_2$ suggests that the extent of Fe-O hybridization DOS is different for M = S and M = Se compounds. The difference in oxygen spectral weight (near 522 eV) $La_2O_2Fe_2O(S,Se)_2$ RIXS spectra may be consistent with resistivity data [Fig. 1(b)] which shows M = S to be a better insulator than M = Se.

In Fig. 2(a), we show the Fe $L_{2,3}$-edge XAS spectra for both $La_2O_2Fe_2OS_2$ and $La_2O_2Fe_2OSe_2$. A magnification (inset)

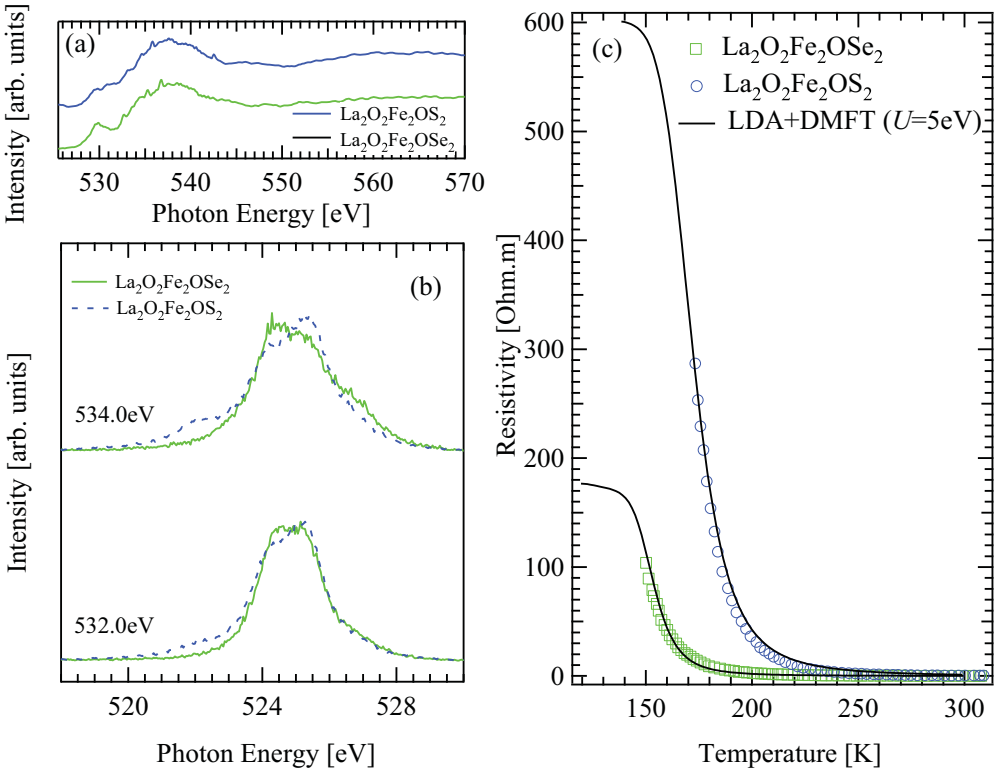

FIG. 1. (Color online) (a) O 1s XAS and (b) O $K\alpha$ RIXS data for $La_2O_2Fe_2OM_2$, (M = S, Se). RIXS intensity data was collected using photons with incident energies of 532 and 534 eV. (c) The electrical resistivity versus temperature T data and the simulated resistivity calculated using LDA + DMFT is shown.

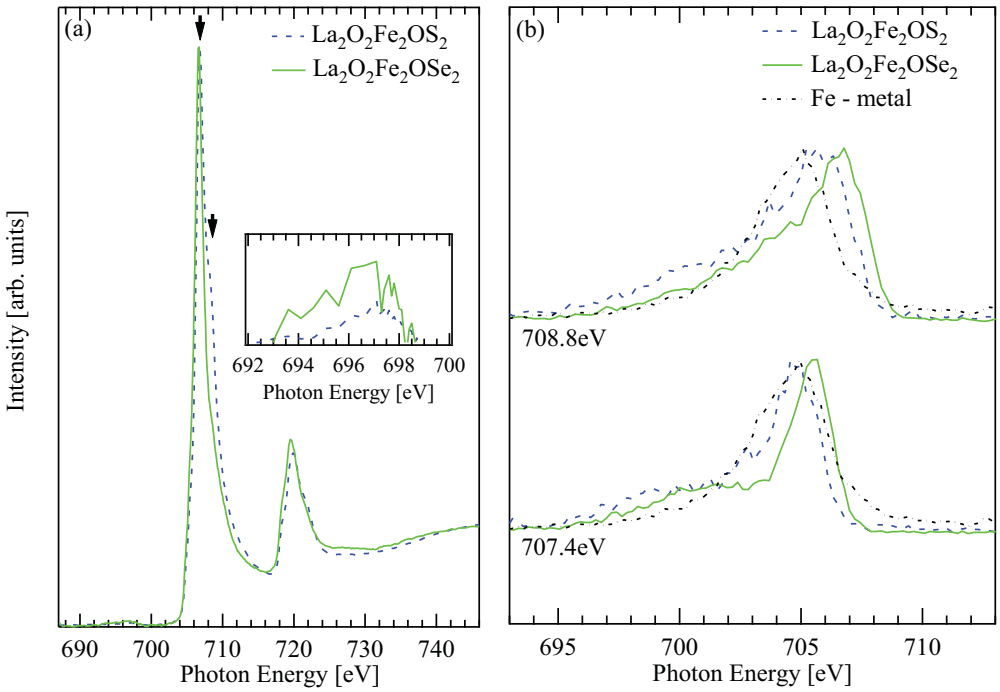

FIG. 2. (Color online) The Fe $L_{2,3}$-edge XAS profiles of $La_2O_2Fe_2OM_2$, (M = S, Se) is shown in panel (a) where the inset contains a magnified view of the upper Hubbard bands. The arrows indicate the x-ray absorption features at the photon energies, 707.4 and 708.8 eV, used to collect the Fe RIXS data in (b). The data are plotted with a vertical offset for clarity.

of the region near the Fermi level, presented in Fig. 2(a), reveal a clear difference in the iron conduction band weight of the two materials. $La_2O_2Fe_2OSe_2$ has enhanced spectral weight at pre-edge just above E_F, and this must ultimately be related to details of the *correlated* electronic structure changes occurring upon replacement of S by Se. Fe XAS data are consistent with both RIXS and bulk measurements that show M = Se to be less strongly correlated than M = S (Appendix A). Resonant inelastic x-ray scattering (RIXS) intensity data [see Fig. 2(b)] were collected using incident x-ray energies tuned to near- and off-resonance Fe x-ray absorption features at 707.4 eV and 708.8 eV, respectively (see Appendix A). RIXS intensity results from a second-order (i.e., two-step) photon-in, photon-out process that can be can be described by the Kramers-Heisenberg (KH) relationship. [15] The KH expression requires the enhancement of the scattering intensity when incident photon energy matches x-ray absorption edge energies. The RIXS data for M = S show correlation-induced broad features in the high-energy spectral region that form the LHB [14,16,17]. In the RIXS data, for both M = S, Se, there is a high intensity Fe 3d metal valence band peak. Near 700 eV, a broad shoulder in the high-energy spectral region is resonantly enhanced. The spectra reveal incoherent electronic excitations involving 3d Fe electrons. These are electron correlation satellites formed by multiparticle excitations among localized Fe states, and indicate the stronger electronic correlations that generate a correlated insulator in the FeO *Ch*.

IV. RESULTS: THEORY

The experimental results above mark the FeO *Ch* as correlated, bandwidth-control driven insulators [18]. The multiorbital FeO *Ch* possess strong interorbital charge transfer, correlations, and crystal field effects all of which make proper characterization of the insulating state a nontrivial issue. To explain the microscopics underlying the experimental data, we performed LDA+DMFT calculations for the FeO *Ch* closely following earlier work [8,11]. LDA calculations were conducted within the linear muffin-tin orbital (LMTO) scheme. The one-electron Hamiltonian reads $H_0 = \sum_{k,a,\sigma} \epsilon_a(k) c^\dagger_{k,a,\sigma} c_{k,a,\sigma}$ with $a = xy, xz, yz, x^2-y^2, 3z^2-r^2$ label (diagonalized in orbital basis) five Fe 3d bands. We retain only the d states, since the non-d orbital DOS have negligible or no weight at E_F. An important aspect of our study is readily visible in Fig. 3 which shows a sizable reduction of the LDA bandwidth relative to that of FeSe (which is itself an incoherent bad metal [19]), induced by hybridization with O states and distorting effects of the La layers. Another interesting aspect, in contrast to Fe arsenides, is that the xz-yz orbital degeneracy in the tetragonal structure is explicitly removed at the outset. Thus, in FeO *Ch*, an electronic nematic (EN) instability linked to ferro-orbital order and its potentially related criticality is not relevant. Finally, clear lower-dimensional band structural features are visible in $\rho^{xz}_{\rm LDA}(\omega)$ (quasi-1D) and $\rho^{xy}_{\rm LDA}(\omega)$ (2D van-Hove singular) near the Fermi energy, $E_F(=0)$. Enhancement of the *effective* U/W ratio in such an intrinsically anisotropic setting should now naturally favor the Mott insulator state in FeO *Ch*. To substantiate this, DMFT calculations were performed using the multiorbital iterated perturbation theory (MO-IPT) as an impurity solver. Though not exact, MO-IPT has a proven record of providing reliable results for a number of correlated systems [20], and is a very efficient and fast solver for arbitrary T and band-filling. The full

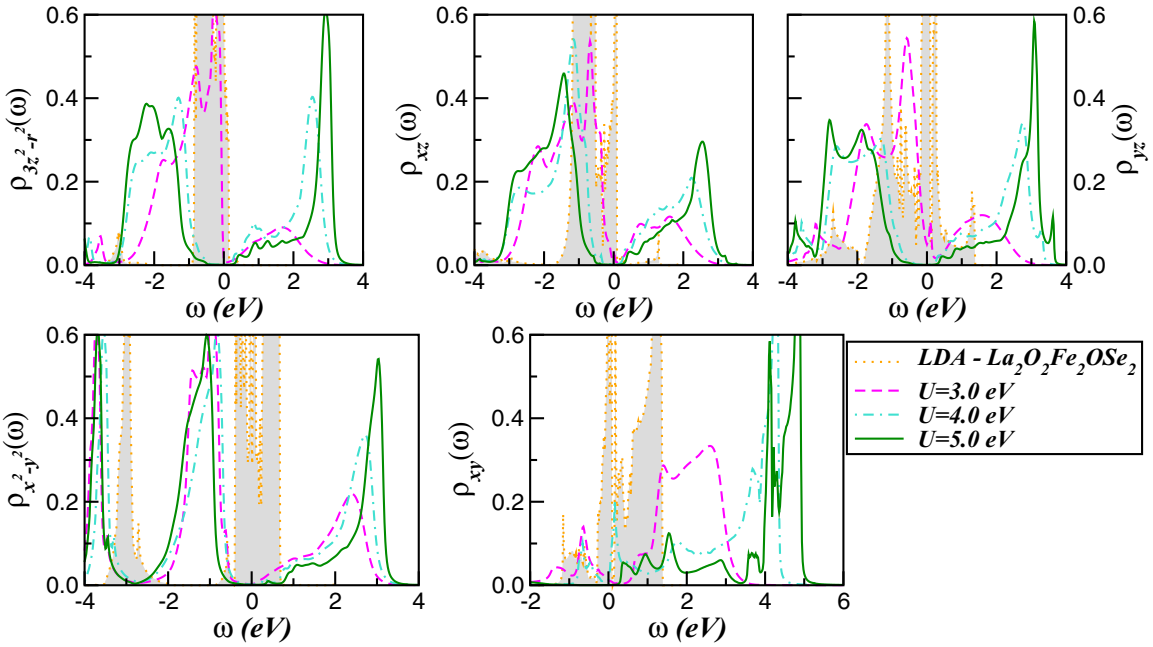

FIG. 3. (Color online) Orbital-resolved LDA density of states (DOS) for the Fe d orbitals of $La_2O_2Fe_2OSe_2$ as well as LDA+DMFT results for different values of U (with $U' = U - 2J_H$) and fixed $J_H = 0.7$ eV. Notice the narrow bands in the LDA DOS. Compared to the LDA results, large spectral weight transfer along with electronic localization is visible in the LDA+DMFT spectral functions for $U \geqslant 4$ eV.

Hamiltonian is $H = H_0 + H_1$ with $H_1 = U \sum_{i,a} n_{ia\downarrow} n_{ia\uparrow} + \sum_{i,a\neq b}[U' n_{ia} n_{ib} - J_H \mathbf{S}_{ia} \cdot \mathbf{S}_{ib}]$, with $U' = (U - 2J_H)$ being the interorbital Coulomb term and J_H the local Hund's coupling. Though $U \simeq 4.0$–5.0 eV and $J_H = 0.7$ eV are expected, we vary $3.0 \leqslant U \leqslant 5.0$ to get more insight.

In Fig. 3, we show the total many-body local spectral function (DOS) for the $M =$ Se case. A clear transition from a bad-metal state at $U = 3.0$ eV to a correlated insulator for $U = 4.0$,5.0 eV occurs. Looking closely at the self-energies in Fig. 4, however, a remarkable aspect stands out: $\mathrm{Im}\Sigma_a(\omega = E_F)$ vanishes in the region of the Mott gap, instead of having a pole, as would occur in a true Mott insulator. This aspect is more reminiscent of a correlated *Kondo* insulator, where the gap arises due to combined effects of electronic correlations and sizable interband hybridization (Appendix B). Thus, the semiconducting behavior of the

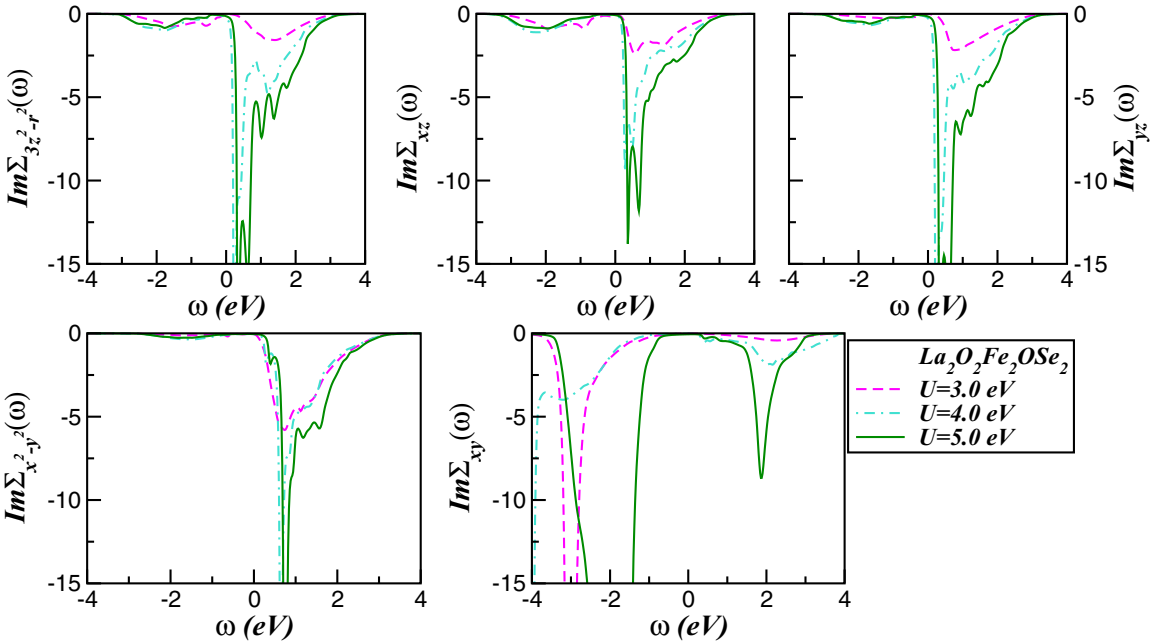

FIG. 4. (Color online) Orbital-resolved imaginary parts of the DMFT self-energies for the Fe d orbitals of $La_2O_2Fe_2OSe_2$ for different values of U and $J_H = 0.7$ eV.

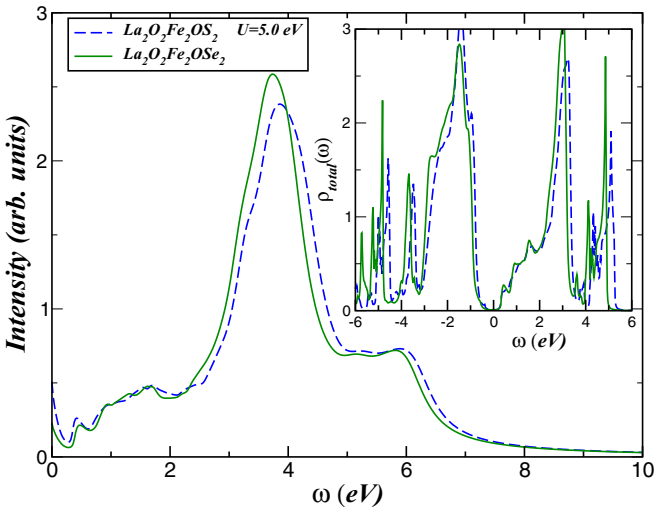

FIG. 5. (Color online) Total LDA+DMFT XAS spectrum of $La_2OFe_2O_2M_2$ (M = S, Se), showing the changes in the upper Hubbard band upon chalcogen substitution matches the behavior observed in the experimental data. Inset shows the corresponding total LDA+DMFT spectral function for $U = 5.0$ eV and $J_H = 0.7$ eV.

$La_2OFe_2O_2M_2$ (M = S, Se) is, in our approach, that of a correlated Kondo insulator. A semiconducting gap opens up because of the orbital-dependent, hybridization-induced Kondo effect, but in contrast to usual band semiconductors, correlation effects in conjunction with band structure details play a crucial role. As is apparent from the orbital-resolved self-energies, correlation effects manifest themselves immediately above the (small) gap scale as sharp pole structures, betraying underlying Mottness in the system. While this finding is somewhat unexpected, proximity to a true Mott state is seen by observing that the pole structures in $\mathrm{Im}\Sigma_a(\omega)$ with $a = xz, yz, 3z^2 - r^2$ lie only slightly above E_F. Thus, because the system *is* correlated, spectral redistribution in response to additional small perturbations (e.g., longer-range Coulomb interactions in an insulator) can drive it into a true Mott insulating phase. More importantly, electron doping will also cause large-scale orbital-selective (see Appendix C) spectral weight transfer, leading to orbital-selective Mott transition (OSMT), wherein a subset of orbital states remain (Mott) gapped in an incoherent metallic state [8]. Such states can exhibit novel quantum criticality associated with an endpoint of the OSMT. Whether HTSC near such novel criticality occurs in suitably doped FeO *Ch* is an open issue.

Figure 5 shows the predicted LDA+DMFT XAS spectra. The relevant effects of core-hole scattering on XAS lineshapes have been incorporated by consistently adapting the procedure of Pardini *et al.* [21] within our DMFT approach. Several important features stand out: (i) There is good semiquantitative agreement with the Fe-edge XAS data up to 3.0 eV above E_F where the predicted spectral weight *differences* between M = S and M = Se closely match the observed spectra. (ii) The theory successfully predicts the smearing of features observed at lower energy ($0.0 < \omega < 2.0$ eV) and higher energy (3.0 eV peak) for M = S relative to M = Se. The prediction of enhanced spectral weight at the pre-edge just above E_F for M = S relative to M = Se agrees with XAS and resistivity data which show M = S to be more correlated than M = Se. Given the LDA+DMFT spectral functions,

$$A_a(\mathbf{k},\omega) = -\frac{1}{\pi}\mathrm{Im}\left[\frac{1}{\omega - \Sigma_a(\omega) - \epsilon_{\mathbf{k},a}}\right]$$

(with $a = xy, xz, yz, x^2 - y^2, 3z^2 - r^2$) the dc resistivity, computed within the Kubo formalism, [22] is expressed exactly [since vertex corrections to $\sigma(T)$ rigorously vanish in DMFT] [23] as $\rho_{\mathrm{dc}}(T) \equiv 1/\sigma(T)$ with

$$\sigma(T) = \frac{\pi}{T}\sum_a \int d\epsilon \rho_a^{(0)}(\epsilon) \int d\omega A_a^2(\epsilon,\omega) f(\omega)[1 - f(\omega)]. \quad (1)$$

Here, $\rho_a^{(0)}(\epsilon)$ is the LDA one-particle density of states (DOS) of the a bands and $f(\omega)$ is the Fermi function. The observed features in $\rho_{\mathrm{dc}}(T)$ must then originate from the spectral changes: Showing how this provides a compelling LDA+DMFT description of experimental data is our focus in this work. LDA+DMFT resistivities (using the Kubo formalism and neglecting vertex corrections to the conductivity [24]), for M = S, Se show very good accord with experiment [where $\rho_{\mathrm{dc}}^{(M)}(T)$ in the PM phase]. This is a strong internal self-consistency check of our proposal.

V. DISCUSSION

We now discuss the implications of our findings for possible HTSC in suitably doped or pressurized systems. Both are expected to tune the Fe-O hybridization: Since we find a correlated Mott-Kondo insulator, this must nontrivially reconstruct the Fe-d states. In $La_2O_2Fe_2OSe_2$, suppression of oxygen Hubbard-band spectral weight presages the onset of bad metallicity even as the localization of the Fe $3d$ states is preserved. This may provide clues to metallize FeO *Ch* by manipulating the oxygen and chalcogen states which hybridize with Fe-d states. This is an exciting perspective because if HTSC results, as in the 245s, it would reinforce the fundamental challenge to the itinerancy perspective in pnictide HTSC research. Specifically, since strong correlations have now obliterated the LDA FS as above, large-scale orbital-selective redistribution of spectral weight upon carrier doping is expected to lead to OSMT and a FS involving only a subset of original d orbitals. The LDA FS and its nesting features would no longer serve as a guide for rationalizing instabilities to order(s). Instead, strong electronic scattering between the partially (Mott) localized and itinerant subsets of the many-body spectral functions generically extinguishes the Landau quasiparticle (QP) pole at E_F. In the absence of a QP description of the normal state, the tenability of the FS nesting scenario is called into question.

We note that the presented results also qualitatively agree with recent findings concerning the nature of magnetism in these systems. Notwithstanding the irrelevance of orbital-correlation driven electronic nematicity in the FeO *Ch*, multiorbital effects indeed seem to be important in this system. The report of anisotropic features, and, in particular, $D = 2$ Ising-like criticality [25] in the AF transition supports an important role in underlying multiorbital electronic hopping processes in the Mott insulator, since these are known [26] to produce $J_1 -$

$J_2 - J_2'$-like spin Hamiltonians with ferromagnetic $J_1(J_2)$ and AF J_2' describing magnetism in Fe-based systems. The small value of the ordered sublattice moment, in contrast to the observed high spin ($S = 2$) on Fe sites, implicates a reduction of the ordered moment due to quantum fluctuations and geometric frustration implied by the spin model above. This involves both orbital fluctuations arising in an effective-Kugel-Khomskii view [27] in a correlated insulator, as well as the sizable frustration with competing (different signs) super-exchanges, arising from multiorbital correlations via the Goodenough-Kanamori-Anderson (GKA) rules. Both coupled spin-orbital physics and frustration now arise from a small t/U expansion in second-order perturbation theory in the setting of the strongly geometrically frustrated multiorbital hopping matrix elements in our multiband Hubbard model.

However, our main point is to suggest that upon suitable doping, AF order will be suppressed. Given the multiorbital physics at work, we also expect an orbital-selective Mott transition (OSMT) to occur around a critical doping level. Such a metal would have no adiabatic connection with the band (LDA) Fermi surface anymore: It generally has no coherent Landau quasiparticles, resulting in bad metallicity and non-FL behavior. In light of widespread occurrence of the maximization of the SC T_c close to such selective-Mott transitions in cuprates and some f-electron-based systems [28], we anticipate a related quantum criticality associated with such a non-FL metallic state to have consequences for possible unconventional superconductivity.

VI. CONCLUSION

Using a combination of experiments and first-principles correlated electronic structure calculations, we present evidence for a novel Mott-Kondo insulator in the FeO *Ch* systems. Agreement between experiment and theory suggest that FeO *Ch* can be tuned into orbital-selective (bad) metals that may be intrinsically unstable to HTSC. In view of similarities to other systems where HTSC is found near doping-induced insulator-to-bad metal transitions, this work provides an impetus to consider likenesses between Fe-based systems and the cuprates. As with the 245 materials, we suggest that FeO *Ch* are ideal candidates for testing this proposal in the Fe-pnictide context. The observed development of incoherent features in XAS and RIXS spectra arises from Mott localized states. If these can be appropriately doped by the manipulation of the Fe-ligand bond by pressurization or appropriate chemical substitution, it is likely that strong orbitally selective scattering will nearly extinguish the Landau-Fermi liquid quasiparticles, leading to the emergence of an incoherent pseudogapped metal reminiscent of underdoped cuprates [8]. Whether novel quantum criticality associated with a selective-Mott transition will be observed with the development of HTSC in FeO *Ch* is of great interest [29]. Our findings provide a compelling motivation to produce and study doped or pressurized iron oxychalcogenides.

ACKNOWLEDGMENTS

The Advanced Light Source (Advanced Photon Source) is supported by the Director, Office of Science, Office of Basic Energy Sciences, of the U.S. Department of Energy (DOE), under Contract No. DE-AC02-05CH11231(DE-AC02-06CH11357). Z.J.U.'s work is supported by the National Basic Research Program of China (973 Program) under Grants No. 2011CBA00103 and No. 2012CB821404, the National Science Foundation of China (Grants No. 11374261 and No. 11204059), and Zhejiang Provincial Natural Science Foundation of China (Grant No. LQ12A04007). M.S.L. thanks MPIPKS, Dresden for hospitality. L.C.'s work was supported by CAPES, Proc. No. 002/2012.L.C. also acknowledges CNPq (Proc. No. 307487/2014-8) and FAPEMAT/CNPq (Project No. 685524/2010), and the Physical Chemistry department at Technical University Dresden for hospitality. We thank Jian-Xin Zhu for initial discussions on this work.

APPENDIX A: MATERIALS AND EXPERIMENT

The iron oxychalcogenide $La_2O_2Fe_2OS_2$, shown in Fig. 6, possesses a structure that is similar to that of the iron pnictides *RE*FeAO (1111) where *RE* = (La, Nd, Sm, Pr, Ce, Gd). However, an oxygen atom in the iron plaquette causes the iron oxychalcogenides (FeO *Ch*) to have a larger Fe unit cell compared to the pnictides. In addition, the *RE* planes of FeO *Ch* contain an oxygen atom. Figure 6 allows a direct comparison of (FeO *Ch*) with $BaFe_2As_2$ (122) and PrFeAsO (1111). The FeO *Ch* are reminiscent of the high-T_c cuprates where a *RE*-O layer separates the transition metal layers. A careful consideration of the FeO *Ch* structure shows that the xz-yz orbital degeneracy, characteristic of the 1111, 11, and 122 Fe pnictides, is absent in this material class. Therefore, the proposals of ferro-orbital order and quantum criticality associated with critical endpoint(s) of electronic nematic transitions are not relevant in the iron oxychalcogenides. These overall similarities and differences make the FeO *Ch* interesting in the context of (i) the intense discussion regarding the amount of correlation in the Fe-based systems, and (ii) the potential observation of HTSC in doped FeO *Ch*.

Synchrotron-based x-ray photons were tuned the O $K\alpha$ (Fe $L_{2,3}$) edges to excite electrons from the O $1s$(Fe $2p$) level, providing direct information on band structural and excitation spectra for Fe-chalcogen layers. It is well accepted that x-ray absorption and emission spectroscopy can be used to measure how the electronic DOS changes as a function of electronic correlation in d- and f-band compounds [15]. Hav-

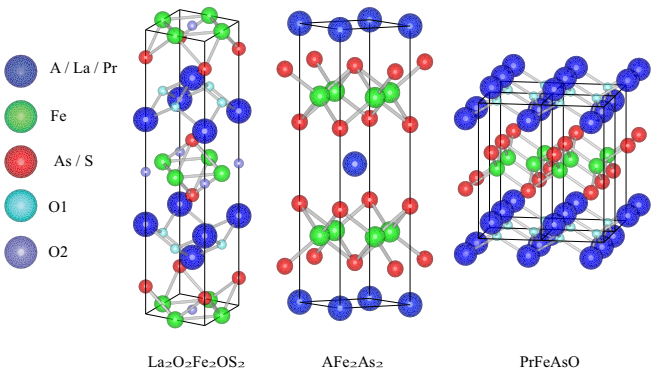

FIG. 6. (Color online) Atomic arrangement of $La_2O_2Fe_2OS_2$, AFe_2As_2 (A = Ba, K, Cs, Sr, and Ca), and PrFeOAs.

ing characterized the DOS of $La_2OFe_2O_2M_2$ ($M = S, Se$) both experimentally and theoretically, we show that a consistent description of observed correlation features (Hubbard bands) mandates that the FeO *Ch* be viewed to have sizable electron correlation. This also suggests that the slightly less correlated 1111, 11, and 122 systems are better described within a similar sizable correlation view, but in a regime with a slightly reduced effective (U/W) ratio, and thus contributes significantly to the debate regarding degree of correlations in Fe-based systems.

In addition, we performed RIXS experiments. In RIXS, the incident x-ray energy is tuned to be equal to that of an absorption edge of a material. Under the resonant condition, it is possible to obtain a resonantly enhanced scattering cross section for the inelastic x-ray scattering processes. This means that spectral features that are excitonic in nature, e.g., collective excitations and many-body interactions can have enhanced spectral intensities which allows them to be detected in the scattered profile. In the main text we present Fe L_3-edge RIXS data from $La_2O_2Fe_2OSe_2$ and $La_2O_2Fe_2OS_2$ that reveal high-energy, correlation-induced excitation features. This spectral weight, shown in Fig. 7, is analogous to a Raman excitation since its intensity and spectral position are dependent on the incident energy of the x-ray photons. Such features are the result of interactions between Mott localized Fe d electrons and represent incoherent spectral weight in the Fe electronic DOS. Figure 7 compares the Fe L_3-edge RIXS data of Fe metal, $BaFe_2As_2$, and $La_2O_2Fe_2O(S,Se)_2$. All three spectra exhibit a dominant fluorescence peak that results from the refilling of the core hole, created during the x-ray absorption process, in the $2p_{3/2}$ state; however, the electron correlation peak structure in FeO *Ch* is not observed in Fe metal or $BaFe_2As_2$.

Using Fe $2p$ XAS, we observe that replacing the S chalcogen with Se leads to the appearance of a prominent upper Hubbard band (UHB) in the Fe $2p$ DOS. We rationalize this within LDA+DMFT (see Fig. 5) in terms of changes in *correlated* electronic structure upon chalcogen replacement.

The O $K\alpha$-edge and Fe L_3-edge RIXS can be understood collectively to show a simultaneous, dual behavior of the $La_2O_2Fe_2O(S,Se)_2$. The Fe correlation behavior is observed to occur in both materials. On the other hand, O RIXS and transport data show that the extent of correlation can be adjusted through chalcogen substitution. The FeO *Ch* appear to accommodate a selectivity of the electron correlation such that some Fe-O states can exhibit correlation-induced spectral while others do not. We understand this effect using LDA+DMFT which indicate that $La_2O_2Fe_2O(S,Se)_2$ exhibit orbital selective Mott insulating behavior. Further, we argue that doping FeO *Ch* should induce orbital-selection Mott-insulator transitions.

APPENDIX B: MOTT-KONDO INSULATING STATE

A correlated Kondo insulator has the following characteristics. Kondo insulators are adiabatically connected to noninteracting semiconductors [30] but are nevertheless strongly correlated systems. Immediately above the hybridization-induced insulating gap, the underlying strongly correlated nature of the (d-band) electronic states manifests itself. Hence,

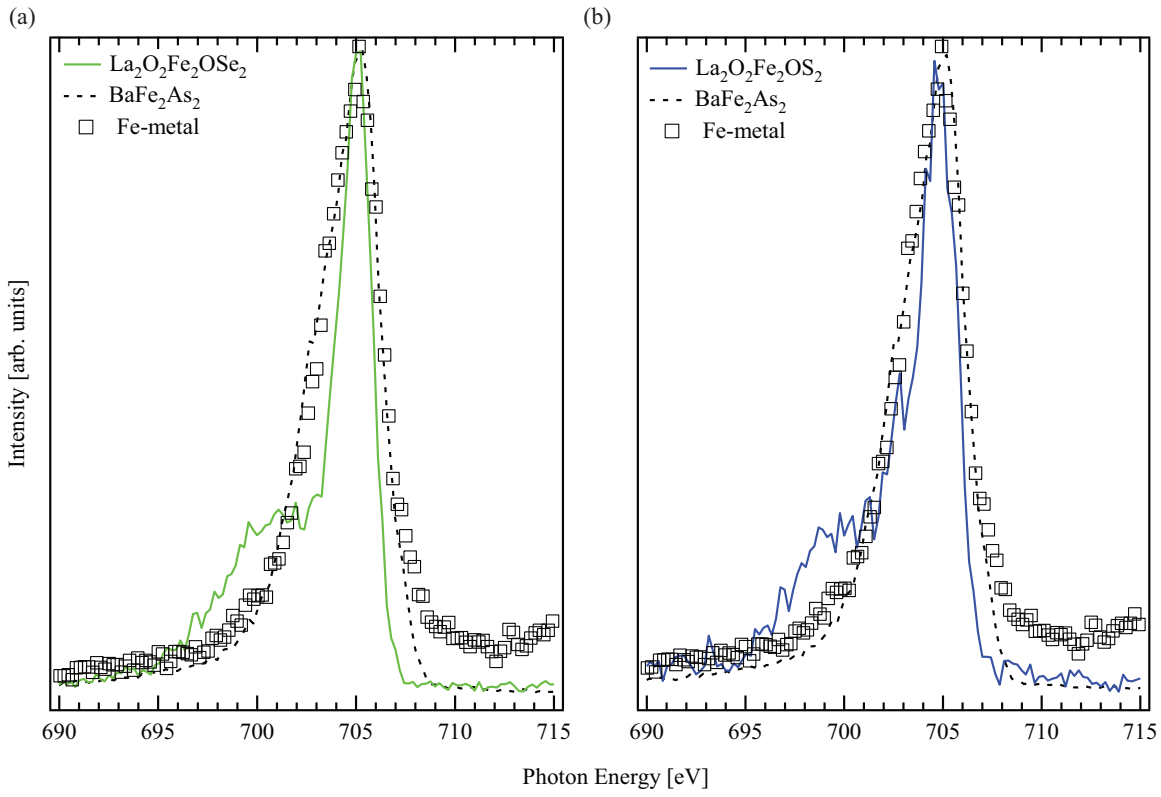

FIG. 7. (Color online) Iron L_3 RIXS spectral profiles of the occupied density of states for (a) $La_2O_2Fe_2OSe_2$ and (b) $La_2O_2Fe_2OS_2$ compared to $BaFe_2As_2$ and Fe metal. High-energy, incoherent spectral weight due to electron correlation is visible in the iron oxychalcogenides. The spectral data were collected using x rays with an incident energy of 707.4 eV.

sizable correlations exist above the one-particle gap scale [31]. On the other hand, in effectively Mott-localized electronic systems the insulating state arises because electron hopping from one site to another is inhibited by strong local Coulomb repulsion. In a Mott insulator (MI), electron hopping is blocked altogether. Doped variants of the MI may result in a metallic state that can vary from an FL to an orbital selective, non-FL depending on the band structural details like crystal-field induced orbital-level splittings, strength of on-site electron-electron interactions, doping, and temperature. According to our LDA+DMFT treatment, the combined Mott-Kondo insulating state in FeO *Ch* arises from the interplay between strong on-site (Mott-Hubbard) and interorbital Coulomb correlations in a system characterized by orbital polarization at the one-particle level. On the other hand, it has been recently realized that interorbital (effectively Falicov-Kimball-like [32] in the selective metal where a coexistence of itinerant and localized d states is found) electronic interactions together with interorbital one-electron hybridization effectively mixes different orbital degrees of freedom, providing a source of correlation-induced hybridization band gaps [33]. Although this insulating state is thus due to the influence of one-electron hybridization and is adiabatically connected to a band insulator, it preserves specific features associated with strong correlations just above the gap. Thus, the insulating features seen in Fig. 3 are indeed linked to strong frequency dependence of $\mathrm{Re}\Sigma_a(\omega)$ (see Fig. 8) in a system with $\mathrm{Im}\Sigma_a(\omega) = 0$ in the gap region as in Fig. 4. While some iron-based superconductors show mixed Mott and Kondo insulating states [11], the insulating state in FeO *Ch* is a true manifestation of a Mott-Kondo insulating state since the hybridization gap is associated with vanishing $\mathrm{Im}\Sigma_a(\omega)$, rather than its divergence, in the region of the insulating gap. The strong energy dependence of the real parts of the orbital-resolved self-energies induces orbital-selective effective electron mass enhancement ($\frac{m^*_\alpha}{m_e} = 1 - \frac{d}{d\omega}\mathrm{Re}\Sigma_\alpha(\omega)|_{\omega=0}$), providing explicit evidence of sizable correlation-induced orbital-selective electronic localization [34] in $La_2OFe_2O_2M_2$ (M = S, Se).

Since we also find that the imaginary parts of the orbital-resolved self-energies have a pole structure very close to $\omega = 0$, it is very conceivable, as discussed in the text, that sizable orbital-selective spectral weight transfer upon suitable doping can lead to an OSMT [33], where a subset of orbital states remain (Mott-like) insulating while the remainder turn metallic. In the generic case, this will lead to bad metallicity and breakdown of the Landau FL picture. Future study should show whether this is obtained in the FeO *Ch*. If it indeed is, it must have far-reaching implications for the instabilities of such an incoherent metal to competing, unconventional orders. Given the lack of one-to-one correspondence between the Fermi surface(s) emerging in such a picture in relation to LDA calculations, this would also preempt traditional "weak-coupling" BCS-like mechanisms for the onset of antiferromagnetism and superconductivity.

APPENDIX C: ORBITAL SELECTIVITY

What is the microscopic origin of the orbital-selective features found in the DMFT solution of $La_2OFe_2O_2M_2$ (M = S, Se) systems? To further clarify this aspect, we recall that in multiorbital (MO) systems, the orbital-resolved hopping matrix elements (diagonalized in the LDA) are sensitive functions of orbital orientation in the real crystal structure. Moreover, the d bands are usually shifted relative to each other because of the action of the crystal field, and the six d electrons in iron-based superconducting materials are distributed among all d orbitals. In the case of $La_2OFe_2O_2M_2$ systems it induces strong orbital polarization within the d-orbital multiplet (see Fig. 3). In this

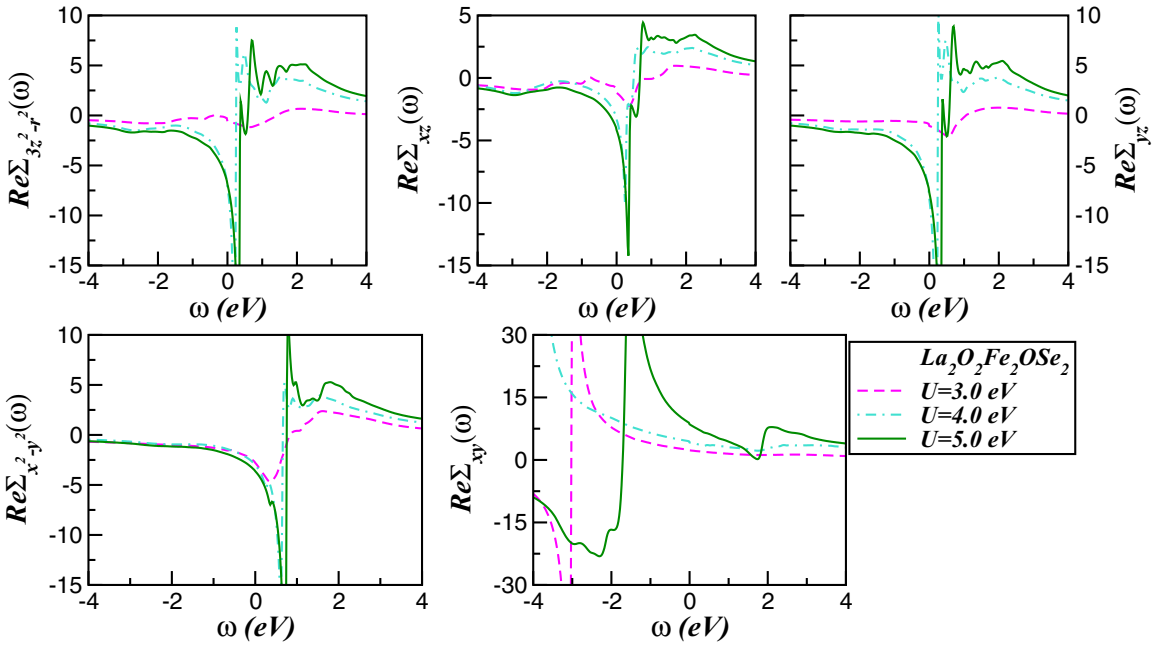

FIG. 8. (Color online) Orbital-resolved LDA+DMFT self-energies (real parts) for $La_2O_2Fe_2OSe_2$, showing dynamical correlation fingerprints in all correlated orbitals. Our results for $U = 5.0$ eV testify a Mott-Kondo insulating state in $La_2O_2Fe_2OSe_2$.

situation, MO correlations cause various intimately linked changes: The static MO Hartree shift, which depends upon the occupations of each orbital as well as on the interorbital correlations [U' and J_H], renormalizes the on-site energies of each orbital in different ways. In particular, it causes interorbital charge transfer between the different d orbitals, self-consistently modifying their energies and occupations [35]. As seen in Fig. 3, the lower-lying orbital(s) in LDA are pushed further up by the MO-Hartree shifts, the amount of which is determined by their occupation(s) and by the values of U,U' relative to their respective LDA bandwidth(s), and to the bare crystal field splittings. As common to strongly correlated electron systems, the dynamical correlations associated with U,U',J_H result in a large-scale transfer of dynamical spectral weight (SWT) accompanying the above changes. When the system is strongly correlated, small changes in the LDA band structure induced by MO electronic correlations (or by changes in external perturbations) induce large changes in SWT, drastically modifying LDA lineshapes. Our XAS and RIXS results for the $La_2OFe_2O_2M_2$ systems bear this expectation very well.

On general grounds, as U,U' increases a subset of d orbitals gets selectively Mott localized. The metallic phase is then the orbital-selective metal found in various contexts [36–38]. Once this selective localization occurs within DMFT, the low-energy physical response is governed by strong scattering between the effectively Mott-localized and the renormalized, itinerant components of the matrix spectral function. The problem is thus effectively mapped onto a generalized spinful Falicov-Kimball [32] type of model, as has been noticed in earlier works [36–38]. Within DMFT, the itinerant fermion spectral function then shows a low-energy pseudogapped form, while the localized spectral function shows a power-law fall-off as a function of energy, as long as the renormalized Fermi energy (E_F) is pinned to the renormalized orbital energy of the localized orbital(s). This is understood from the mapping of the corresponding impurity model to that of the "x-ray edge" [39], where the orthogonality catastrophe destroys Fermi liquid behavior [40]. The spectral functions then exhibit asymmetric continuua at low energy, instead of symmetric Abrikosov-Suhl Kondo resonance features at low energies, and the metallic phase is non-Fermi liquid.

A strong coupling method as used here will yield the antiferromagnetic (AF) ordered ground state at low temperatures, in analogy with one-band Hubbard model studies, where the AF ordered state at half-filling remains the Néel ordered state, evolving from Goodenough-Kanamori-Anderson [20] type of interactions. However, our findings for the paramagnetic Kondo-Mott insulating state are in accord with an earlier MO LDA+DMFT work [8], which was the first to recognize the realistic strong coupling aspect of Fe-oxychalcogenides. As shown here, the frequency dependence of the self-energy implies stabilization of the Kondo-Mott insulating state, and consideration of the instability of such a state to a metallic or to a superconducting (SC) state leads to a fully reconstructed Fermi surface (which preempts a weak-coupling starting point) and to a strongly frequency-dependent superconducting gap function. (We plan to explore these aspects in future works on the Fe-oxychalcogenides family.)

[1] Y. Kamihara, T. Watanabe, M. Hirano, and H. Hosono, Iron-Based Layered Superconductor La[$O_{1-x}F_x$]FeAs (x = 0.05–0.12) with Tc = 26 K, J. Am. Chem. Soc. **130**, 3296 (2008).

[2] Q. Si and E. Abrahams, Strong Correlations and Magnetic Frustration in the High T_c Iron Pnictides, Phys. Rev. Lett. **101**, 076401 (2008).

[3] M. R. Norman, High-temperature superconductivity in the iron pnictides, Physics **1**, 21 (2008).

[4] A. V. Chubukov, D. V. Efremov, and I. Eremin, Magnetism, superconductivity, and pairing symmetry in iron-based superconductors, Phys. Rev. B **78**, 134512 (2008).

[5] G. Baskaran, Lafeaso as a self doped spin-1 Mott insulator: Quantum string liquid state and superconductivity, J. Phys. Soc. Jap. **77**, 113713 (2008).

[6] T. Imai, K. Ahilan, F. L. Ning, T. M. McQueen, and R. J. Cava, Why does undoped FeSe become a high-T_c superconductor under pressure? Phys. Rev. Lett. **102**, 177005 (2009).

[7] J.-X. Zhu, R. Yu, H. Wang, L. L. Zhao, M. D. Jones, J. Dai, E. Abrahams, E. Morosan, M. Fang, and Q. Si, Band Narrowing and Mott Localization in Iron Oxychalcogenides $La_2\mathbf{O}_2Fe_2\mathbf{O}(Se,\mathbf{S})_2$, Phys. Rev. Lett. **104**, 216405 (2010).

[8] L. Craco, M. S. Laad, and S. Leoni, Orbital-selective Mottness in layered iron oxychalcogenides: the case of $Na_2Fe_2OSe_2$, J. Phys.: Condens. Matter **26**, 145602 (2014).

[9] M.-H. Fang, H.-D. Wang, C.-H. Dong, Z.-J. Li, C.-M. Feng, J. Chen, and H. Q. Yuan, Fe-based superconductivity with T_c =31 k bordering an antiferromagnetic insulator in (Tl,K) Fe_xSe_2, Europhys. Lett. **94**, 27009 (2011).

[10] J. M. Mayer, L. F. Schneemeyer, T. Siegrist, J. V. Waszczak, and B. Van Dover, New layered iron-lanthanum-oxide-sulfide and -selenide phases: $Fe_2La_2O_3E_2$(E = S,Se), Angewandte Chemie International Edition in English **31**, 1645 (1992).

[11] L. Craco, M. S. Laad, and S. Leoni, Unconventional Mott transition in $K_xFe_{2-y}Se_2$, Phys. Rev. B **84**, 224520 (2011).

[12] D. G. Free and J. S. O. Evans, Low-temperature nuclear and magnetic structures of $La_2O_2Fe_2OSe_2$ from x-ray and neutron diffraction measurements, Phys. Rev. B **81**, 214433 (2010).

[13] F. M. F. de Groot, M. Grioni, J. C. Fuggle, J. Ghijsen, G. A. Sawatzky, and H. Petersen, Oxygen 1s x-ray-absorption edges of transition-metal oxides, Phys. Rev. B **40**, 5715 (1989).

[14] E. Z. Kurmaev, R. G. Wilks, A. Moewes, N. A. Skorikov, Y. A. Izyumov, L. D. Finkelstein, R. H. Li, and X. H. Chen, X-ray spectra and electronic structures of the iron arsenide superconductors $\mathbf{R}FeAsO_{1-x}F_x$($\mathbf{R}$ = La,Sm), Phys. Rev. B **78**, 220503 (2008).

[15] A. Kotani and S. Shin, Resonant inelastic x-ray scattering spectra for electrons in solids, Rev. Mod. Phys. **73**, 203 (2001).

[16] V. I. Anisimov, E. Z. Kurmaev, A. Moewes, and I. A. Izyumov, Strength of correlations in pnictides and its assessment by theoretical calculations and spectroscopy experiments, Physica C **469**, 442 (2009).

[17] A. Koitzsch, R. Kraus, T. Kroll, M. Knupfer, B. Büchner, H. Eschrig, D. R. Batchelor, G. L. Sun, D. L. Sun, and C. T. Lin, Observation of two-hole satellite in the resonant x-ray photoemission spectra of $Ba_{1-x}K_xFe_2As_2$ single crystals, Phys. Rev. B **81**, 174519 (2010).

[18] M. Imada, A. Fujimori, and Y. Tokura, Metal-insulator transitions, Rev. Mod. Phys. **70**, 1039 (1998).

[19] L. Craco, M. S. Laad, and S. Leoni, Low-temperature metal-insulator transition in the electron-doped iron chalcogenide FeSe superconductor, Europhys. Lett. **91**, 27001 (2010).

[20] A. Georges, G. Kotliar, W. Krauth, and M. J. Rozenberg, Dynamical mean-field theory of strongly correlated fermion systems and the limit of infinite dimensions, Rev. Mod. Phys. **68**, 13 (1996).

[21] L. Pardini, V. Bellini, and F. Manghi, Effects of electronic correlation on x-ray absorption and dichroic spectra at l 2, 3 edge, J. Phys.: Condens. Matter **23**, 215601 (2011).

[22] K. Haule and G. Kotliar, Coherence—incoherence crossover in the normal state of iron oxypnictides and importance of Hund's rule coupling, New J. Phys. **11**, 025021 (2009).

[23] A. Khurana, Electrical conductivity in the infinite-dimensional Hubbard model, Phys. Rev. Lett. **64**, 1990 (1990).

[24] J. M. Tomczak and S. Biermann, Multi-orbital effects in optical properties of vanadium sesquioxide, J. Phys.: Condens. Matter **21**, 064209 (2009).

[25] E. E. McCabe, C. Stock, E. E. Rodriguez, A. S. Wills, J. W. Taylor, and J. S. O. Evans, Weak spin interactions in Mott insulating $La_2O_2Fe_2OSe_2$, Phys. Rev. B **89**, 100402 (2014).

[26] P. Phillips, T.-P. Choy, and R. G. Leigh, Mottness in high-temperature copper-oxide superconductors, Rep. Prog. Phys. **72**, 036501 (2009).

[27] K. I. Kugel and D. I. Khomskii, Crystal structure and magnetic properties of substances with orbital degeneracy, Sov. Phys. JETP **37**, 725 (1973).

[28] T. Park, F. Ronning, H. Q. Yuan, M. B. Salamon, R. Movshovich, J. L. Sarrao, and J. D. Thompson, Hidden magnetism and quantum criticality in the heavy fermion superconductor CeRhin5, Nature (London) **440**, 65 (2006).

[29] G. Giovannetti, L. de' Medici, M. Aichhorn, and M. Capone, $La_2O_3Fe_2Se_2$: A Mott insulator on the brink of orbital-selective metallization, Phys. Rev. B **91**, 085124 (2015).

[30] M. Dzero, K. Sun, V. Galitski, and P. Coleman, Topological Kondo Insulators, Phys. Rev. Lett. **104**, 106408 (2010).

[31] L. Craco, Quantum orbital entanglement: A view from the extended periodic Anderson model, Phys. Rev. B **77**, 125122 (2008).

[32] L. M. Falicov and J. C. Kimball, Simple Model for Semiconductor-Metal Transitions: SmB_6 and Transition-Metal Oxides, Phys. Rev. Lett. **22**, 997 (1969).

[33] V. Stanev and P. B. Littlewood, Nematicity driven by hybridization in iron-based superconductors, Phys. Rev. B **87**, 161122 (2013).

[34] Q. Yin, A. Kutepov, K. Haule, G. Kotliar, S. Y. Savrasov, and W. E. Pickett, Electronic correlation and transport properties of nuclear fuel materials, Phys. Rev. B **84**, 195111 (2011).

[35] M. S. Laad, L. Craco, S. Leoni, and H. Rosner, Electrodynamic response of incoherent metals: Normal phase of iron pnictides, Phys. Rev. B **79**, 024515 (2009).

[36] S. Biermann, L. de' Medici, and A. Georges, Non-Fermi-Liquid Behavior and Double-Exchange Physics in Orbital-Selective Mott Systems, Phys. Rev. Lett. **95**, 206401 (2005).

[37] M. S. Laad, L. Craco, and E. Müller-Hartmann, Orbital Switching and the First-Order Insulator-Metal Transition in Paramagnetic V_2O_3, Phys. Rev. Lett. **91**, 156402 (2003).

[38] M. S. Laad, L. Craco, and E. Müller-Hartmann, Orbital-selective insulator-metal transition in V_2O_3 under external pressure, Phys. Rev. B **73**, 045109 (2006).

[39] P. W. Anderson, Infrared Catastrophe in Fermi Gases with Local Scattering Potentials, Phys. Rev. Lett. **18**, 1049 (1967).

[40] M. Combescot and P. Nozières, Infrared catastrophy and excitons in the x-ray spectra of metals, J. Phys. France **32**, 913 (1971).